A new method to overall immobilization of phosphorus in sediments through combined application of capping and oxidizing agents

Qin Sun [a,*], Juan Lin [b,c], Jingxin Cao [b,c], Cai Li [b,d], Dan Shi [b,d], Mingrui Gao [a], Yan Wang [e], Chaosheng Zhang [f], Shiming Ding [b,e,**]

[a] Key Laboratory of Integrated Regulation and Resource Development on Shallow Lakes, Ministry of Education, College of Environment, Hohai University, Nanjing 210098, China
[b] State Key Laboratory of Lake Science and Environment, Nanjing Institute of Geography and Limnology, Chinese Academy of Sciences, Nanjing 210008, China
[c] University of Chinese Academy of Sciences, Beijing 100049, China
[d] School of Water Conservancy and Environment, University of Jinan, Jinan 250022, China
[e] Nanjing EasySensor Environmental Technology Co., Ltd., Nanjing 210018, China
[f] International Network for Environment and Health, School of Geography and Archaeology, National University of Ireland, Galway, Ireland

HIGHLIGHTS

- Combined capping-oxidizing treatment had significant advantages over the individual treatments.
- SRP in the overlying water were only 10%, 21% and 4% for the CK, LMB and CN treatments.
- Immobilization P effect reached from the SWI to a depth of 60 mm in the sediment.
- Ammonia nitrogen concentrations in the pore water eventually returned to the normal level.

GRAPHICAL ABSTRACT
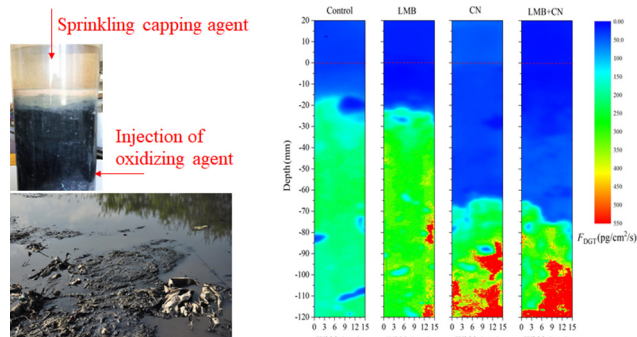
ARTICLE INFO

ABSTRACT

A new method has been developed for improving the overall immobilization efficiency of phosphorus (P) in sediment. A capping agent (lanthanum modified bentonite, LMB) was sprinkled on the sediment surface to prevent the release of P in the top sediment layer. Meanwhile, an oxidizing agent (calcium nitrate, CN) was injected into the sediment layer (~5 cm) to immobilize labile P in deep sediment layers. High-resolution sampling techniques, including diffusive gradients in thin films (DGT) and high-resolution dialysis (HR-Peeper) were employed to investigate the fine-scale changes of labile and/or soluble nitrogen, P, sulfide and iron in sediments, respectively. The results showed that the combined application of LMB and CN had significant advantages over the individual treatments. The average concentrations of soluble reactive phosphorus (SRP) (0.01 mg/L) in the overlying water after a 68-day incubation were only 10%, 21% and 4% for the CK, LMB and CN treatments, respectively. Furthermore, the immobilization effect caused by the combined treatment reached from the sediment-water interface to a depth of 60 mm in the sediment, and the effective depth was much >20 mm caused by LMB treatment. The concentrations of SRP in the sediment profile were also lower than those of the other treatments. The results

* Corresponding author.
** Correspondence to: S. Ding, State Key Laboratory of Lake Science and Environment, Nanjing Institute of Geography and Limnology, Chinese Academy of Sciences, Nanjing 210008, China.
E-mail addresses: sunqinnj@hhu.edu.cn (Q. Sun), smding@niglas.ac.cn (S. Ding).

of this work indicate that the combined application of capping and oxidizing agents is a promising method to control water eutrophication by preventing the release of P from both the top and deep sediment layers.

1. Introduction

In-situ immobilization technique is a commonly used method to control the release of phosphorus (P) from sediments in eutrophic lakes (Wang and Jiang, 2016). Its principle is to convert mobile P in sediments into P in more stable forms by adding active materials (Wang et al., 2014). Mobile P fractions can be stabilized and solidified through chemical adsorption, flocculation, precipitation, or chemical reaction between chemical materials and P in various forms in sediments (Lurling et al., 2014). There are many *in-situ* immobilization materials, mainly including aluminum salt (Lurling et al., 2016; Rydin et al., 2017), iron salt (Kowalczewska-Madura et al., 2017), calcium salt (Dittrich et al., 2011; Liu et al., 2009), lanthanum modified bentonite (LMB) (Copetti et al., 2016; Spears et al., 2016), nitrate (Xu et al., 2014; Yamada et al., 2012), waste mud of water plants (Wang et al., 2016), new modified materials (Wang et al., 2018; Zhang et al., 2017) and combination of various materials (Lurling et al., 2017; Waajen et al., 2017).

LMB is formed by ion exchange between lanthanum and ions in bentonites. It is a kind of bentonite modified by lanthanum containing about 5% lanthanum (Meis et al., 2013). LMB was originally developed as P (mainly orthophosphate) adsorbent for the treatment of eutrophic waterbodies and was put into production by Australian CSIRO Institution in 1990s. At present, LMB is one of the most commonly used materials in P control research and is used in >200 waterbodies around the world, including eutrophic fish ponds, rivers and lakes, of which about 50% are distributed in Europe, 30% in Australia and New Zealand, 15% in North America and the rest in Asia, Africa and North America (Copetti et al., 2016). However, it was also found that the use of LMB was not effective in some lakes, such as Het Groene Eiland Lake in the Netherlands (Lurling and van Oosterhout, 2013). Lang et al. (2016) studied the effects of LMB treatment in Loch Flemington Lake (United Kingdom) and found that the eutrophication of the lake was not improved and the cyanobacteria bloom was not controlled after the addition of LMB for two years. Reasons for the inefficiency of LMB may include the effects of resuspension or cyanobacteria deposition, the impacts of redox conditions, pH, alkalinity and dissolved organic carbon (DOC) on the adsorption of P by LMB and the addition of insufficient amount of LMB for controlling P (Copetti et al., 2016).

Since Ripl's first report, calcium nitrate treatment has been considered as a feasible technology for *in-situ* remediation of sediments (Foy, 1986; Ripl, 1976). The basic principle of nitrate treatment technique is to stimulate denitrification by adding nitrate, to degrade organic matter, to reduce the chemical energy of loose degradable organic matter, to oxidize reduced FeS to iron-oxygen (hydrogen-oxygen) compounds (FeOOH) and to absorb phosphate in pore water. When the chemical energy of organic matter is low to a certain extent, mobile P in sediment can be fixed (Feibicke, 1997). Nitrate can easily dissolve in lake water, and its solubility is several orders of magnitude higher than that of oxygen. Therefore, nitrate permeates more easily into sediments than oxygen, and consequently, the range of oxidized iron produced by nitrate is larger (Hansen et al., 2003). At present, the research on calcium nitrate treatment involves many aspects, such as black-odor treatment (Shao et al., 2011; Zhang et al., 2009), endogenous P control (Yamada et al., 2012), and organic pollutants remediation (Cunningham et al., 2001; Hutchins et al., 1998). Many studies have shown that adding calcium nitrate to promote denitrification is an economical and effective method to treat the black-odor problem in sewage, oil storage and

sediments (Garcia-de-Lomas et al., 2007; Jiang et al., 2009; Shao et al., 2011; Wang et al., 2016). In simulation experiments, nitrate successfully suppressed the release of P in sediments in East Lake, China (Lin et al., 2017; Liu et al., 2009), Upper Mystic Lake, USA (Hemond and Lin, 2010), Vedsted Lake, Denmark (Hansen et al., 2003), Ibirite Reservoir, Brazil (Yamada et al., 2012), and other lakes (Bostrom and Pettersson, 1982; Na and Park, 2004; Tiren and Pettersson, 1985).

During the immobilization process, the slow release of potential P sources in sediments weakens the effects of remediation (Wang et al., 2016). In order to solve this problem, increased dosage or repeated addition of immobilization agents is required in lakes (Kleeberg et al., 2013; Meis et al., 2013). However, overdose in a single addition would have an adverse impact on the water ecological environment (Gołdyn et al., 2014). Furthermore, repeated application is bound to increase the cost of treatment. Therefore, the development of combination technologies with low dose, high P fixation capability and stable P fixation effect is the focus and hot spot of current research. Although the P controlling effect of LMB is stable, its influence range on endogenous P in sediments is limited to 1–2 cm of surface layer and it cannot stabilize the bottom P (Wang et al., 2017). Calcium nitrate can significantly affect the stability of P in the deep sediment layers, but may have poor controlling effect on the release of P in the top sediment layer (Lin et al., 2015; Lin et al., 2017). Therefore, combined use of LMB and calcium nitrate has the potential to overcome the defects of the respective agents and to have better control over the P release from sediments.

In this study, sediment simulation experiment was conducted to investigate the effects of single and combination applications of LMB and calcium nitrate on the release of P from sediments. High-resolution sampling techniques including diffusive gradients in thin films (DGT), high-resolution dialysis (HR-Peeper) and microelectrode were used to investigate the fine-scale changes of several targets, such as dissolved and/or labile nitrogen, P and iron in sediments under different treatments. The effects of different application methods on the release of P from sediments were compared and the mechanisms involved in the processes were explored.

2. Materials and methods

2.1. Materials

LMB was provided by Fusiyueke LLC (Sichuan, China). The LMB sample was ground and passed through a 2 mm pore-size mesh before use. HR-Peeper and DGT probes were provided by Easysensor Ltd. (Nanjing, China). The probes were deoxygenated using nitrogen for 16 h prior to use. Water and sediment samples used for incubation experiments were collected from the Nanfei River input to Lake Chaohu (the fifth largest freshwater lake in China) in Anhui Province, China (117.401° N, 31.717° E). Sediment column samples were collected with cylindrical sampler, and the bottom was sealed with rubber plug. The water and sediment properties have been reported elsewhere (Wang et al., 2017).

2.2. Experimental core microcosm set-up

The sediment cores were sectioned at 2 cm interval. All the sediment sections taken at the same depth were mixed and homogenized, followed by removal of large particles and macrofauna through a mesh of 0.6 mm pore size. The sediment samples were placed in 16 Perspex tubes according to their original depths to form a 14 cm thickness

sediment core. The water samples were filtered through a 0.45 μm ni-trocellulose filter (Millipore). Then, they were siphoned into the sediment core tube, and the thickness of the water layer was about 15 cm. Four sediment cores were selected for insertion of Rhizon samplers. The samplers were installed at the depth of 0 (the position of the sediment-water interface; SWI), −10 (the minus denotes the position below the SWI), −20, −30, −40 and −60 mm in sediments. All the sediment core tubes were deployed in a water bath at 25 °C for one month, and the water layer was replenished every 2–3 days.

The sediment cores were divided into 4 groups, and each group was treated according to four methods, including the control without addition of any agents (abbreviated as CK), application of LMB, application of calcium nitrate (CN), combined application of LMB and calcium nitrate (LMB + CN). For the LMB treatment, LMB was evenly sprinkled on the sediment surface. The application dose of LMB was 120 LMB/P$_{mobile}$ (the molar ratio of the amount of LMB to that of mobile P in the surface 4 cm sediments) (Wang et al., 2017). The content of P$_{mobile}$ was determined according to the scheme developed by Rydin and Welch (1999). For the CN treatment, calcium nitrate (Ca(NO$_3$)$_2$·4H$_2$O) was mixed with filtered lake water and injected into the sediment at the depth of −5 cm. The dose of calcium nitrate application was 45.3 g N/m^2, which was lower than that reported by Yamada et al. (2012). For the LMB + CN treatment, calcium nitrate was first injected into the sediments followed by application of LMB according to the same methods and dosages as mentioned earlier.

Pore waters in sediments were collected at intervals of hours or days (once before adding treatment agents, 0 h). About 0.8 mL of pore water was collected by Rhizon sampler at each time point, and dissolved iron, dissolved nitrate nitrogen and ammonia nitrogen, and SRP, were determined immediately after collection. The pH, DO and conductivity at the depth of 30 mm in the overlying water were measured regularly. On day 67 after treatment, the pH and redox state were measured using micro-electrode (Unisense, Denmark). Zr-oxide and AgI DGTs were used to measure labile P and sulfide (S(-II)) in the sediment-water profiles on two-dimensional, submillimeter levels. ZrO-Chelex DGT was used to measure labile Fe on one-dimensional, millimeter level. All three DGTs were inserted vertically into the sediments, leaving about 2 cm above the SWI. The DGT device was removed 24 h after it was inserted into the sediments. The surface of the DGT probes was washed with deionized water and then the probe was placed into a clean self-sealing bag before analysis.

2.3. Analytical methods

The DO concentration and conductivity of the overlying water were measured by an oxygen dissolving instrument (Leici JPB-607A, Shanghai) and a conductivity meter (Leici DDB-303A, Shanghai), respectively. The pH of the overlying water was measured by a portable pH meter (Leici PHBJ-260, Shanghai). The SRP and dissolved iron were determined by molybdenum blue and phenanthroline colorimetric methods, respectively (Murphy and Riley, 1962; Tamura et al., 1974). The concentrations of NO$_3^-$-N, NH$_4^+$-N and NO$_2^-$-N were determined by ultraviolet, salicylic acid-hypochlorite, and N-(1-naphthyl)-ethylenediamine spectrophotometric methods, respectively (Lu, 1999).

The Zr-oxide gel retrieved from the Zr-oxide gel DGT was colorated in a mixed molybdenum reagent at 35 °C for 45 min. The concentration of DGT-labile P was then determined by a computer imaging densitometry (CID) technique (Ding et al., 2013). The surface of the AgI binding gel was directly scanned to obtain the grayscale intensity, and the concentration of DGT-labile sulfide was further determined by a CID technique (Ding et al., 2012). The ZrO-Chelex binding gel was sliced at intervals of 4 mm. Each slice was eluted for Fe using 1.0 M HNO$_3$. The concentration of Fe was determined using the phenanthroline colorimetric method mentioned earlier.

2.4. Data analysis

The grayscale images of the AgI and colorated Zr-oxide gel surfaces were converted to P or S(-II) cumulative quantity (M) using the calibration curves established before (Ding et al., 2012, 2013). Then, the labile P or S(-II) was calculated as the flux of P or S(-II) (F_{DGT}) by using Eq. (1) (Li et al., 2019),

$$F_{DGT} = M/At \qquad (1)$$

where M represents the cumulative amount of P or S(-II), A represents the exposed area of the fixed film, and t represents the deployment time of the DGT device in sediments.

The DGT-labile Fe was interpreted as the time-averaged concentration at the probe interface (C_{DGT}), as shown by Eq. (2) (Li et al., 2019):

$$C_{DGT} = \frac{M\Delta g}{DAt} \qquad (2)$$

where Δg is the thickness of the diffusion layer (cm); D is the analyte diffusion coefficient in the diffusion layer (cm^2·s^{-1}); t is the deployment time (s); A is the gel exposure area (cm^2); and M is the corresponding accumulated mass over the deployment time (μg).

The obtained flux or concentration data were plotted by Origin 8 software, and the difference between the different treatments was analyzed by independent sample t-test (SPSS v19.0). The significance level was $p < 0.05$.

3. Results and discussion

3.1. Variation of sediment appearance

The visible appearance of sediments after injection of calcium nitrate at the depth of −50 mm is shown in Fig. 1. An oxide layer with a thickness of about 20 mm existed at the SWI before the injection of calcium nitrate. On the 0.5th and 1.5th day, the variation of sediment appearance was not significant. On the 2.5th day, a light color appeared at −120 to −150 mm depth of the sediment. On the 4th day, the light-colored region expanded and the thickness of surface oxide layer increased to about 50 mm. During the 4th to 13th days, the thickness of the oxide layer increased with time. On the 13th day, the range of the light-colored region expanded to 180 mm from the surface layer. During the 13th to 69th days, there was no obvious change in the appearance of the sediment. After treatment for 69 days, the sediment core could be divided into three layers according to the appearance: light tan layer at 0 to −70 mm, light gray-black layer at −70 to −180 mm, and black layer below −180 mm. Similar phenomena were observed by Hansen et al. (2003) and Yamada et al. (2012), where the black sediment turned yellow-orange after 34 days of sodium nitrate treatment or 145 days of calcium nitrate treatment, respectively.

3.2. Changes in conductivity, pH and redox state

The variation of pH, DO concentration and conductivity in the overlying water after treatments is shown in Fig. 2. On the 44th day, the pH of the overlying water after LMB + CN treatment was significantly lower than that after LMB treatment ($p < 0.05$), and there was no significant difference from that after CK treatment. On the 11th day and 68th day, there was no significant difference in pH between the different groups ($p > 0.05$). On the 11th day, the DO concentration after LMB treatment was significantly lower than the other groups, and there was no significant difference between the groups on the 44th and 68th days. On the 44th day, there was a significant difference in conductivity between the groups, which could be ranked from small to large as follows: LMB + CN treatment > CN treatment > LMB treatment > CK treatment. On the 68th day, there was no significant difference in the conductivity between LMB treatment and CK treatment, while the
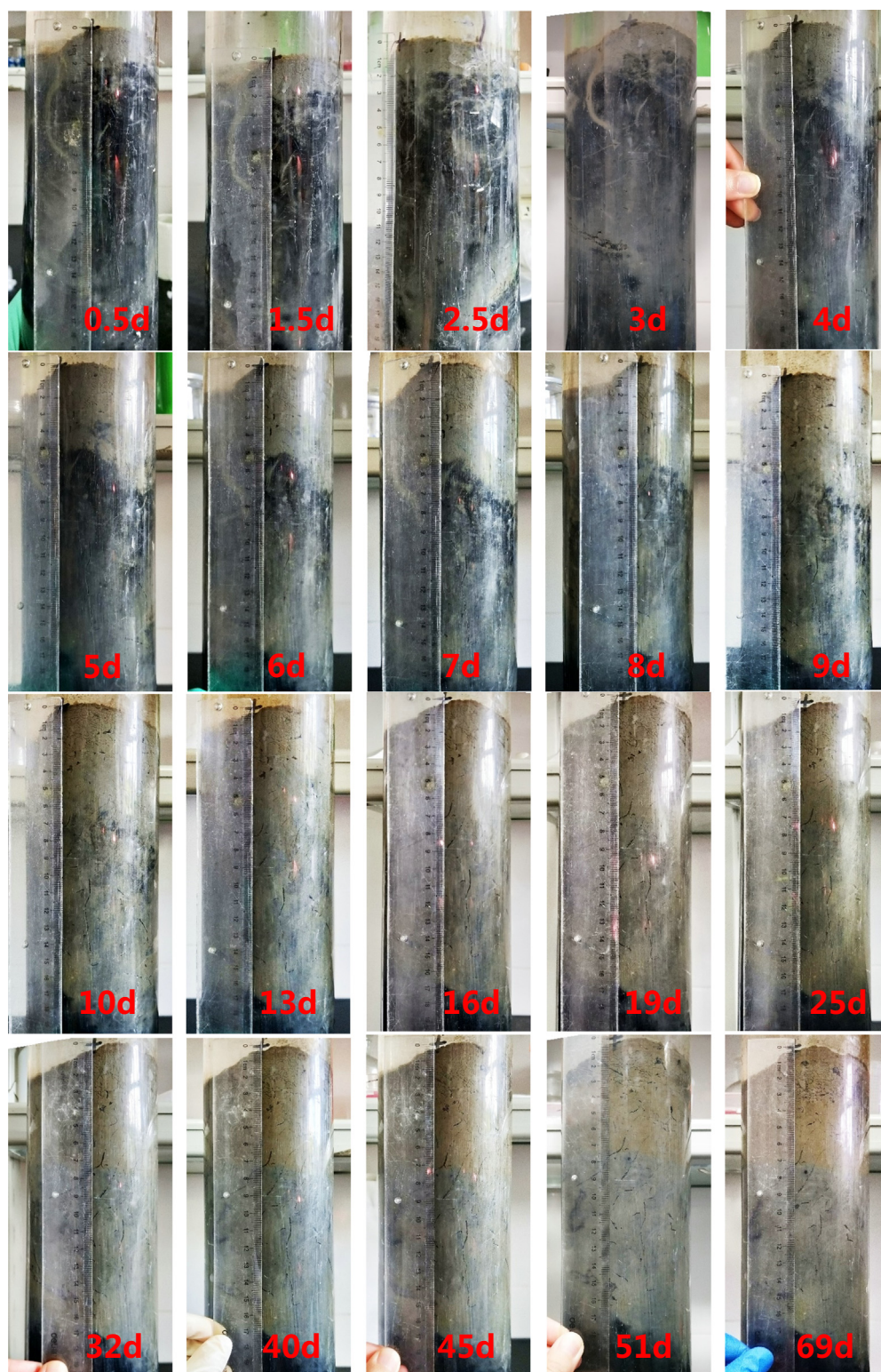
Fig. 1. Variation of the appearance of sediment profiles after combined application with lanthanum modified bentonite and calcium nitrate.

conductivity after CK treatment was significantly higher compared to the other groups. The conductivity after CN treatment was significantly higher than that after CK and LMB treatments.

The variation of pH and redox state in the sediment-water profiles after 67 days treatment is shown in Fig. 3. There was no significant difference in pH between the CK, LMB and CN treatments ($p > 0.05$). There was no significant difference in pH between LMB + CN treatment and CK treatment at 5 to −1.5 mm depths, while the difference was significantly lower than that after CK treatment at −2 to −19 mm depths. The pH after LMB + CN treatment was
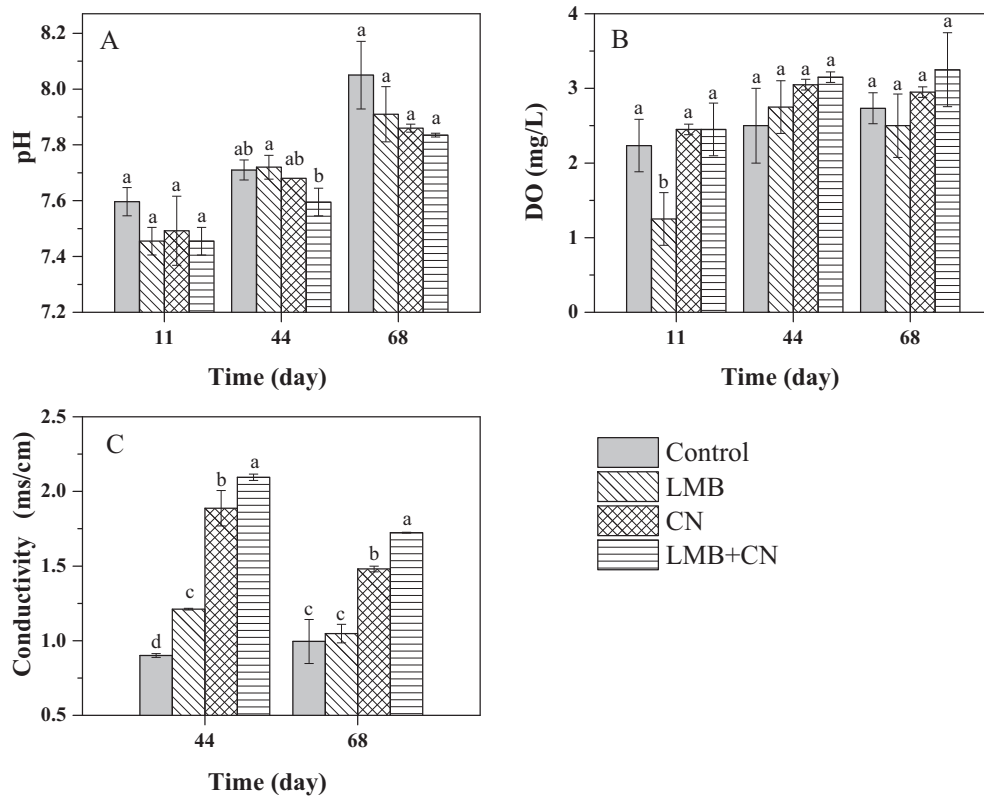
Fig. 2. Variation of (A) pH, (B) DO and (C) conductivity in the overlying water after different treatments for 68 days (the significant differences are labelled with lowercase letters and p < 0.05).

significantly lower than that after LMB treatment at −8.5 to −13.5 mm depths, which was significantly lower than that after CN treatment at −8.5 to −15.5 mm depths.

The Eh value after LMB treatment was significantly higher than that after CK treatment at 5 to −2.5 mm depths ($p < 0.05$), and there was no

significant difference between LMB treatment and CK treatment at −2.5–30 mm depths ($p > 0.05$). Eh values after CN treatment and LMB + CN treatment were significantly higher than the corresponding values after CK treatment at 5 to −30 mm depths. Eh value after CN treatment was significantly higher than that after LMB treatment at
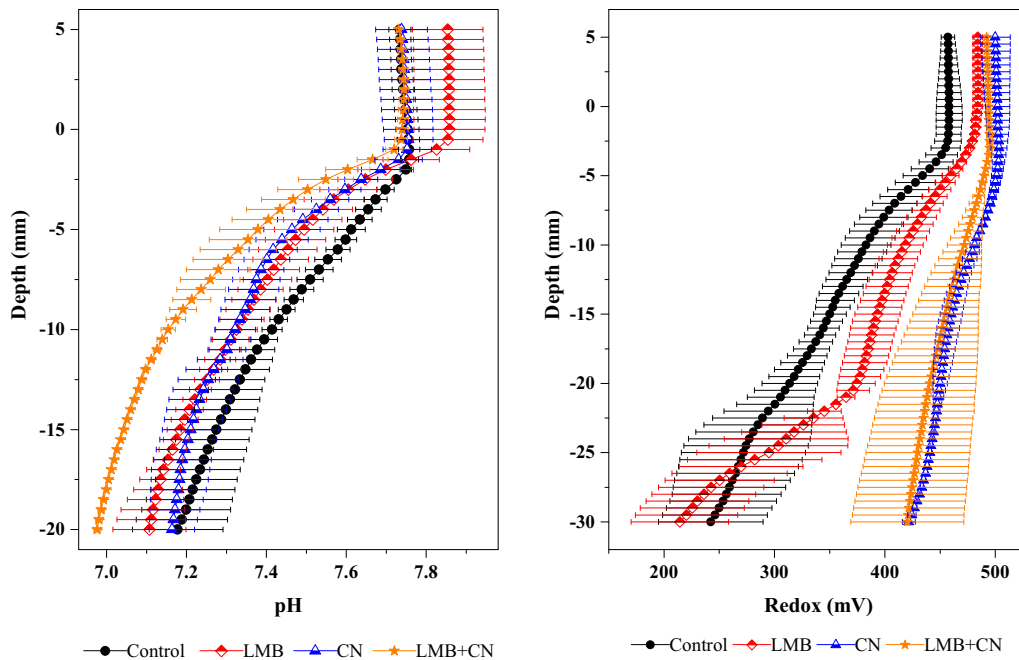

Fig. 3. Variation of pH and redox state (Eh) in the sediment-water profiles after different treatments for 67 days.

−2 to −30 mm depths. Moreover, Eh after LMB + CN treatment was significantly higher than that after LMB treatment at −4.5 to −30 mm depths.

3.3. Changes in nitrogen

The changes in NO_3^--N concentrations in pore water with time after the four treatments are displayed in Fig. 4. The concentrations of NO_3^--N in pore water after CK treatment were in the range of 1.80–2.53 mg/L, and there was no significant difference between 0 and 68 days. In addition, the NO_3^--N concentrations after LMB treatment had no significant difference compared to CK treatment. The nitrogen concentrations increased sharply at 2 h after CN treatment and LMB + CN treatment. The concentration of NO_3^--N increased to 594–1390 mg/L after CN treatment, and the maximum and minimum concentrations were at −20 mm and −60 mm depths, respectively. At 2 h, the NO_3^--N concentration after LMB + CN treatment was much higher than that after CN treatment at −40 mm. This could be because the Rhizon sampler just collected the pore water at the injection point of $Ca(NO_3)_2$ solution. The concentration of NO_3^--N after LMB + CN treatment decreased

rapidly at −40 mm, and the injected $Ca(NO_3)_2$ solution at 4–12 h gradually spread to other zones.

From 4 h to 68 days, the concentration of NO_3^--N after CN treatment and LMB + CN treatment showed decreasing trends overall, with some intermittent increases. For example, the concentrations increased at −30, −40 and −60 mm around the 10th day. On the 9th day, it was observed that the NO_3^--N concentration at −30 mm after LMB + CN treatment decreased to 2.40 mg/L, and increased to 13.08 mg/L on the 10th day. The NO_3^--N concentration decreased to 2.78 and 1.36 mg/L at −40 mm on 9th and 10th days after CN treatment and LMB + CN treatment, respectively, but then the concentration increased again. On the 8th day, the NO_3^--N concentration after CN treatment and LMB + CN treatment decreased to 1.97 and 1.80 mg/L at −60 mm, respectively, following a slight increase. On the 68th day, the NO_3^--N concentrations after CN treatment were 17.51, 6.90, and 2.80 mg/L at the depths of 30, 40, and −60 mm, respectively. The corresponding values were 29.32, 10.77, and 3.41 mg/L after LMB + CN treatment, respectively. These results suggested that NO_3^--N in the surface pore water continued to diffuse into the deep layers, and the sediments at −30, −40, and −60 mm had the ability to consume the injected and diffused NO_3^--N to the pretreatment level.
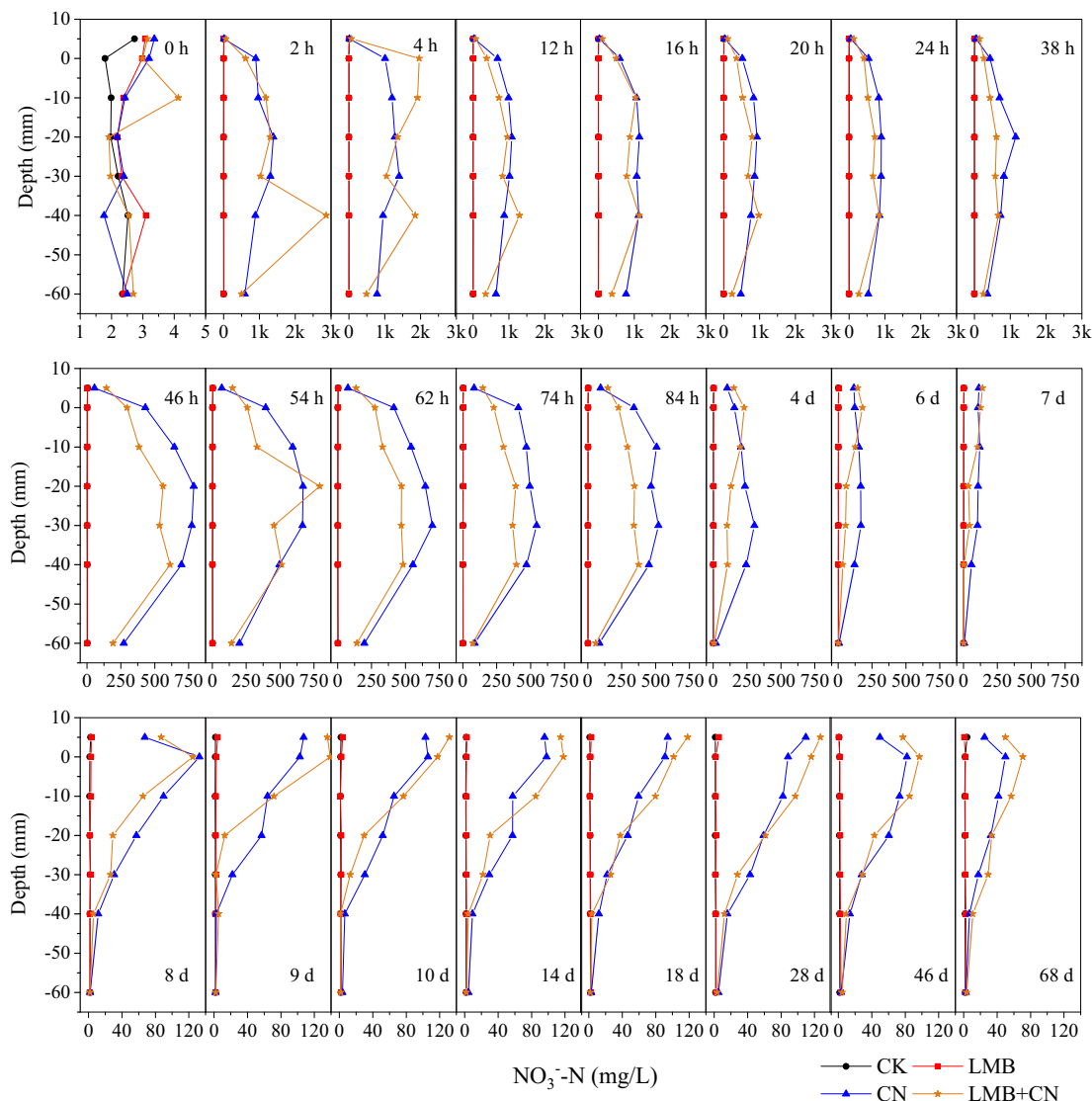

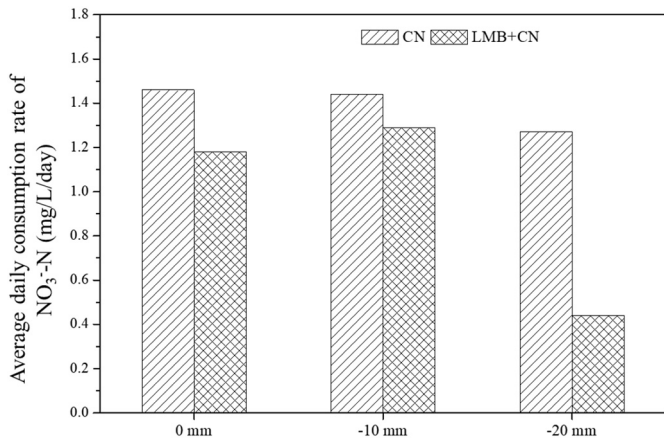Fig. 4. Changes in concentrations of soluble nitrate nitrogen with time in sediment-water profiles.

Fig. 5. Average daily consumption rate of NO_3^--N in different depths of sediments from the 46th to 68th day.

On the 68th day, the NO_3^--N concentrations after CN treatment were 49.83, 41.65, and 32.39 mg/L at depths of 0, −10, and −20 mm, respectively, and the corresponding values after LMB + CN treatment were 70.85, 56.88, and 33.50 mg/L, respectively. The average daily consumption rate was calculated from the NO_3^--N concentrations after CN treatment and LMB + CN treatment from the 46th to 68th day, and the results are shown in Fig. 5. The average consumption rate of NO_3^--N after CN treatment was 1.27–1.46 mg/L/day, and that after LMB + CN treatment was 0.44–1.29 mg/L/day. Thus, it can be inferred that at day 68, the concentrations of NO_3^--N were still decreasing at 0, −10 and −20 mm, and the injected NO_3^--N was still being consumed. Based on the consumption rate at the 68th day, it was necessary to continue the incubation for 34 days, and the added NO_3^--N could be completely consumed after CN treatment. After 76 days of incubation, the added NO_3^--N was completely consumed after LMB + CN treatment. In addition, the simulation experiment was limited by experimental conditions, and the height of the overlying water was only 20 cm, which was far less than the actual water depth in the lake. In practical applications, the concentration of NO_3^--N in the overlying water will be much lower than the simulation experiment due to the dilution of water flow. Therefore, in the actual situation, whether NO_3^--N can be restored to the pretreatment level after CN and LMB + CN treatments still needs further verification by experiments.

The changes in NH_4^+-N concentrations in pore water with time after the four different treatments are displayed in Fig. 6. Before the
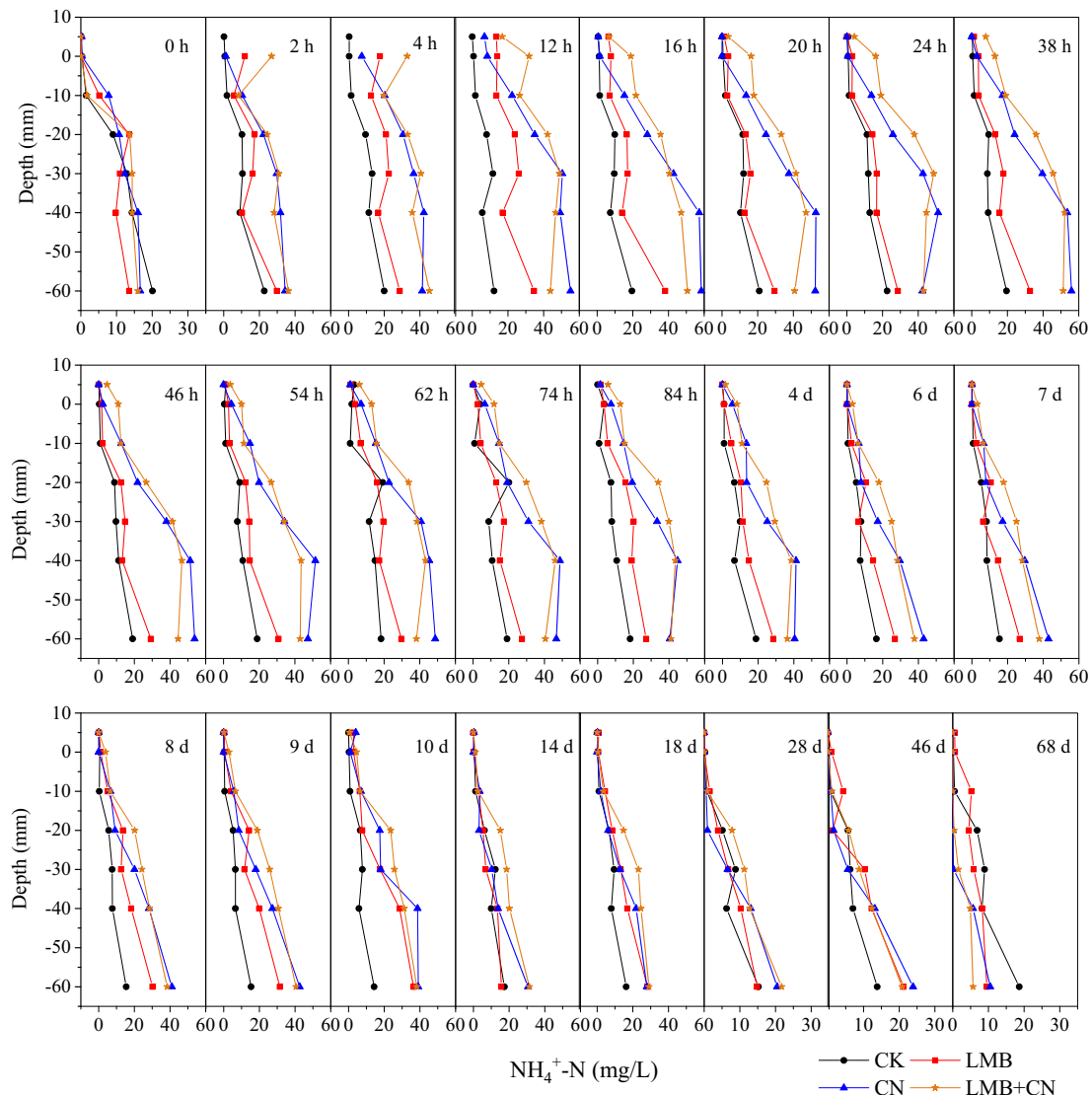

Fig. 6. Changes in concentrations of soluble ammonia nitrogen with time in sediment-water profiles.

incubation of CK treatment (0 h), the NH_4^+-N concentrations in pore water increased with the depth and were in the range from 0.34 to 20.10 mg/L. The NH_4^+-N concentrations after LMB, CN and LMB + CN treatments rapidly increased at 2 h. LMB treatment and LMB + CN treatment showed the largest increase at 0 mm, indicating that LMB may contain NH_4^+-N. At 12 h, the NH_4^+-N concentrations after LMB treatment were 13.94, 13.49, 23.88, 26.11, 17.07 and 34.60 mg/L at the depths of 0, −10, −20, −30, −40 and −60 mm, respectively. Furthermore, the NH_4^+-N concentrations were 0.67, 5.22, 4.49, 5.89, 8.23, and 9.59 mg/L on the 68th day at these depths, respectively, and there were no significant differences compared with the CK treatment. The concentrations of NH_4^+-N after CN treatment increased with time from 0 to 16 h, and the concentration in the deeper region increased more than that in the surface layer. The NH_4^+-N concentrations at the 16th hour were 8.39, 22.34, 34.97, 50.45, 49.26 and 55.12 mg/L, respectively. From 20 h to 68th day, the NH_4^+-N concentrations decreased with time, and were 0, 0, 0, 0.23, 5.69, and 10.52 mg/L on day 68. These values are much lower compared to the corresponding values for CK treatment. The concentration of NH_4^+-N increased with time from 0 to 38 h during LMB + CN treatment, and the peak values were 13.08, 19.07, 36.14, 45.67, 52.15 and 51.26 mg/L, respectively. NH_4^+-N concentrations

gradually decreased with time from 38 to 68 days, and decreased to 0, 0, 0.36, 1.59, 4.94 and 5.67 mg/L on day 68. The concentration of NH_4^+-N after LMB + CN treatment was much smaller than that after CK treatment.

The enrichment of NH_4^+-N in water bodies and its toxicity to aquatic organisms has received increasing attention (Rao et al., 2018; Yan et al., 2019; Zhuang et al., 2019). Studies have shown that the accumulation of excessive ammonia nitrogen can reduce the carbohydrate and starch contents of aquatic plants and inhibit plant growth (Cao et al., 2007; Rao et al., 2018; Zhuang et al., 2019). In ammonia nitrogen-rich waters, aquatic plant leaves tend to absorb NH_4^+-N rather than nitrogen (Nichols and Keeney, 1976), and continue to absorb NH_4^+-N even after absorbing the amount needed to sustain plant growth. To avoid excessive enrichment in the body, plant tissues synthesize excess NH_4^+-N into other nitrogen compounds (such as free amino acids) or transport them out of the tissue. These processes can consume large amounts of sugars and energy and inhibit the synthesis of biomass (Cao et al., 2007; Yuan et al., 2013). In this study, NH_4^+-N in the pore-water after LMB, CN and LMB + CN treatments increased over a short period of time (about 11 days). However, after 68 days of treatment, the NH_4^+-N concentration returned to a lower level. The NH_4^+-N concentrations
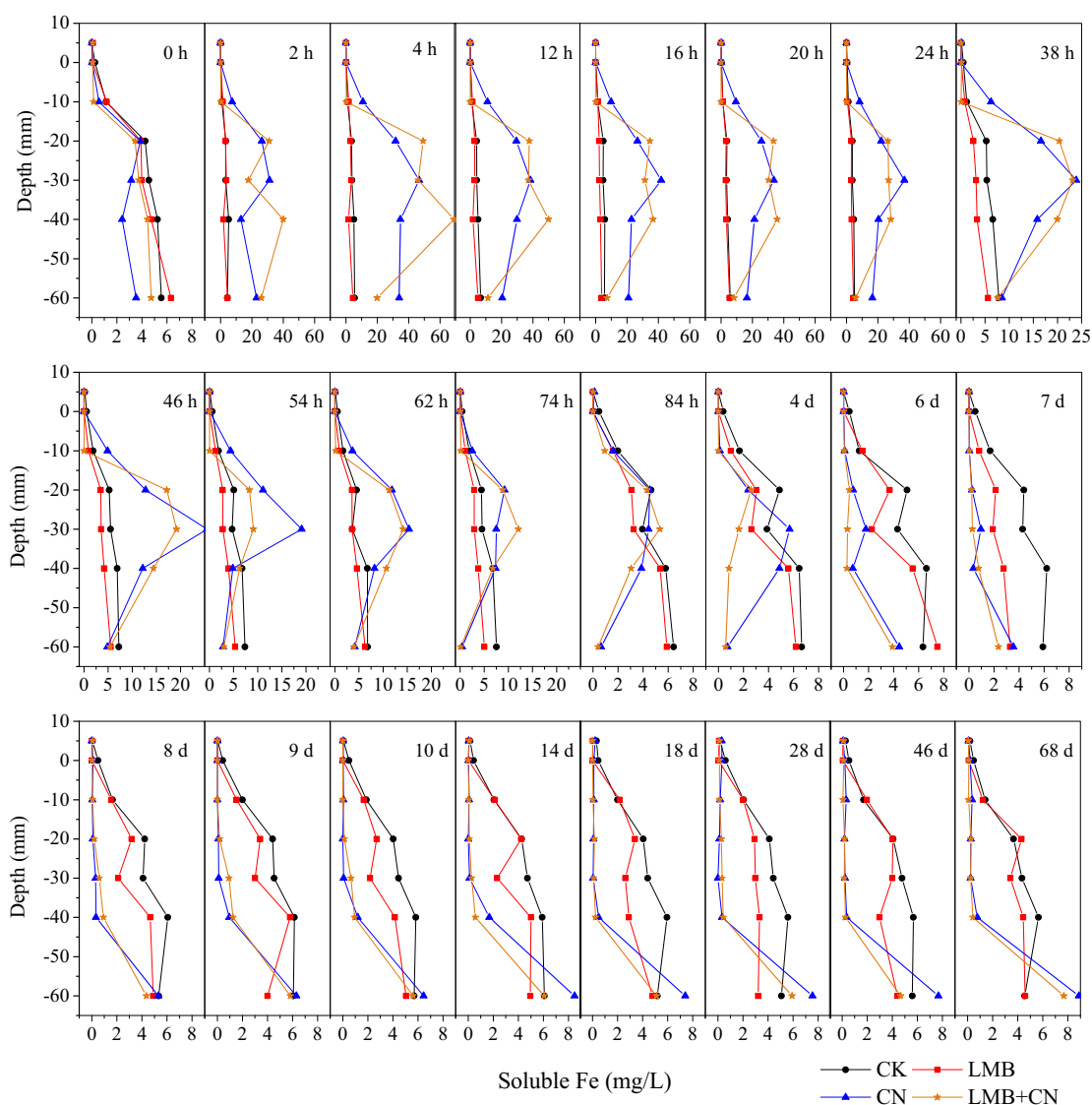

Fig. 7. Changes in concentrations of soluble Fe with time in sediment-water profiles.

after CN treatment and LMB + CN treatment were even lower than that of the control.

3.4. Changes in sediment Fe

Fig. 7 presents the changes of soluble Fe in pore water after the four treatments. At the control treatment, the concentrations of soluble Fe increased with the increase in depth, from 0.26 to 5.55 mg/L between 0 and −60 mm. Compared to the control, LMB treatment reduced the concentration of soluble Fe after 24 h treatment. The largest difference appeared on the 7th day, when the average concentration of soluble Fe decreased from 4.21 to 1.88 mg/L. This was likely caused by the adsorption of Fe^{2+} ion by LMB. The adsorption capacity of 8.51 mg/g was obtained through batch adsorption experiments (Ding et al., 2018). After the addition of $Ca(NO_3)_2$, the concentration of soluble Fe increased slightly, but was still lower than that of the control at the SWI (0 mm). It gradually increased from −10 to −60 mm with the maximum value varying from 11.07 to 46.75 mg/L, and decreased with time from 12 h to 68 days. The concentrations of soluble Fe were 0.25 to 8.88 mg/L at the 68th day from −10 to −40 mm, which were lower than those after CK treatment. After LMB + CN treatment, the concentrations of soluble Fe increased slightly with increase in time at the SWI, but remained lower than those of the control treatment. The concentration of soluble Fe reduced to 0.09 mg/L at −10 mm depth, and first increased and then decreased with time from −20 to −60 mm. Its maximum value ranged from 26.05 to 68.94 mg/L, which decreased to 0.25–7.68 mg/L at the 68th day.

Fig. 8 shows the vertical distribution of DGT-labile Fe after the different treatments for 68 days. For all treatments, the concentrations of DGT-labile Fe remained at a low level from 10 to −15 mm, and there

Fig. 8. Change of DGT-labile Fe in the sediment-water profiles after the four treatments for 68 days.

were no obvious differences between different treatments. The concentrations were obviously lower than those of the control treatment from 0 to −65 mm. The average values of DGT-labile Fe concentrations decreased to 0.066 and 0.056 mg/L at the depths of −25 and −60 mm. There was no obvious difference among different treatments from −70 to −80 mm.

After the addition of $Ca(NO_3)_2$, nitrate is used as electron receptor to oxidize sulfur participating in iron sulfide precipitation. Consequently, Fe (II) would be released, which would then be oxidized, and eventually form FeOOH (which can bind to phosphate) (Yamada et al., 2012). This process directly resulted in the decrease in concentrations of soluble and DGT-labile Fe in the sediment as observed earlier (Figs. 7–8). On the other hand, a part of Fe in sediment exist in the form of stable and insoluble Fe sulfides in anoxic sediments. Sulfides in sediments, also known as acid volatile sulfides (AVS), are very sensitive to oxidation environment. When sulfides are oxidized by nitrate, sulfide-associated metals, such as Fe, Cu, Cd, Zn, Pb and Ni, can be activated and released into pore water and overlying water (De Jonge et al., 2012). This was demonstrated by the increases of soluble Fe concentrations in pore water at the early incubation period (up to 84 h) (Fig. 7).

3.5. Changes in sulfide

The changes in DGT-labile S(II) fluxes in the sediment-water profiles after 68 days of different treatments are presented in Fig. 9. The DGT-labile S(II) after LMB treatment was significantly higher than that after CK treatment. This was likely due to the decrease in soluble Fe(II) adsorbed by LMB (Fig. 7), resulting in less Fe(II) to bind with and precipitate S(II). The DGT-labile S(II) fluxes after CN treatment and LMB + CN treatment were significantly lower compared to CK treatment at 0 to −65 mm and 0 to −75 mm, respectively, and the flux was close to 0. The addition of $Ca(NO_3)_2$ significantly affected the circulation of sulfur in the sediment, which oxidized the reduced sulfur, resulting in an increase in the concentration of SO_4^{2-}. This was consistent with the previous research on the treatment of black odorous wastewater by $Ca(NO_3)_2$. After adding $Ca(NO_3)_2$ to the wastewater, most or all of the sulfides were quickly removed, producing a large amount of SO_4^{2-}. The N/S ratio was correlated with the formation of SO_4^{2-} (De Lomas et al., 2006; Watsuntorn et al., 2019). There are similar reports on the use of $Ca(NO_3)_2$ to treat black odorous sediments. Feibicke (1997) found that the concentrations of SO_4^{2-} in the overlying water and interstitial water were significantly reduced by injecting $Ca(NO_3)_2$ into a fjord sediment in Germany. Xu et al. (2014) applied 45.3 g N/m² of $Ca(NO_3)_2$ three times in river sediments, and found that the concentration of SO_4^{2-} in pore-water increased from 3.59 mg/L to 17.55 mg/L after 96 h. In surface sediments, the sulfide content was significantly reduced. These findings suggested that $Ca(NO_3)_2$ treatment can significantly ameliorate the black odor of water and sediment problem.

3.6. Change in phosphorus

Fig. 10 shows the variation of SRP with time in pore water of sediments. Before the incubation, the concentrations of SRP ranged from 0.17 to 3.08 mg/L, and the maximum and minimum values existed at the depths 0 and −30 mm, respectively. However, after LMB treatment, the concentration of SRP decreased nearly to 0 at the depth of 0 mm, and did not increase during the experimental duration. At the depth of −10 mm, the concentration of SRP increased from 0 to 12 h, and then decreased from 12 to 46 h. Its value was 2.32 mg/L at the 68th day, which was higher than that of the control treatment. At the deeper layer from −20 to −60 mm, SRP fluctuated with no significant increasing or decreasing trends. Compared to the control treatment, there was no obvious difference. These results indicate that the LMB dosage used in this experiment could control SRP in pore water up to a depth <10 mm below the SWI. For the single group after $Ca(NO_3)_2$ treatment, the concentration of SRP only slightly changed, at the depth of 0 mm,

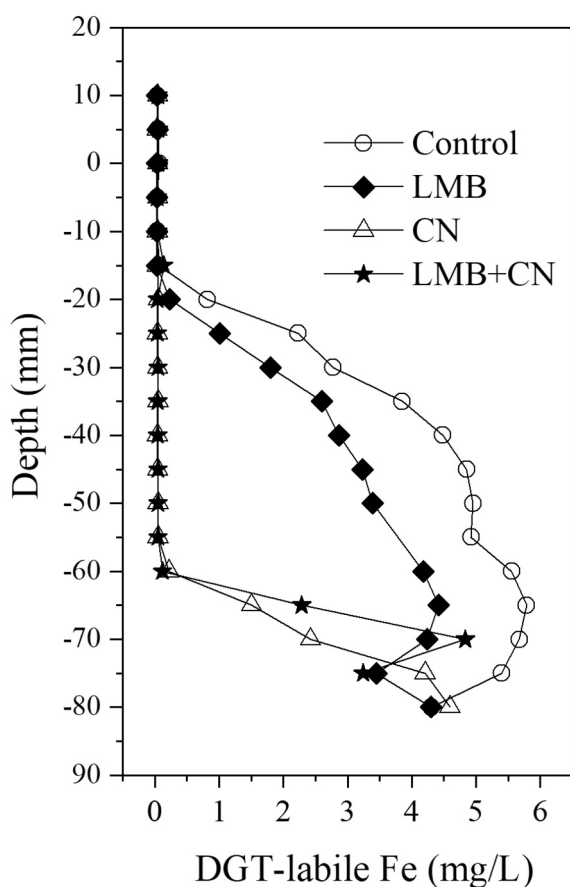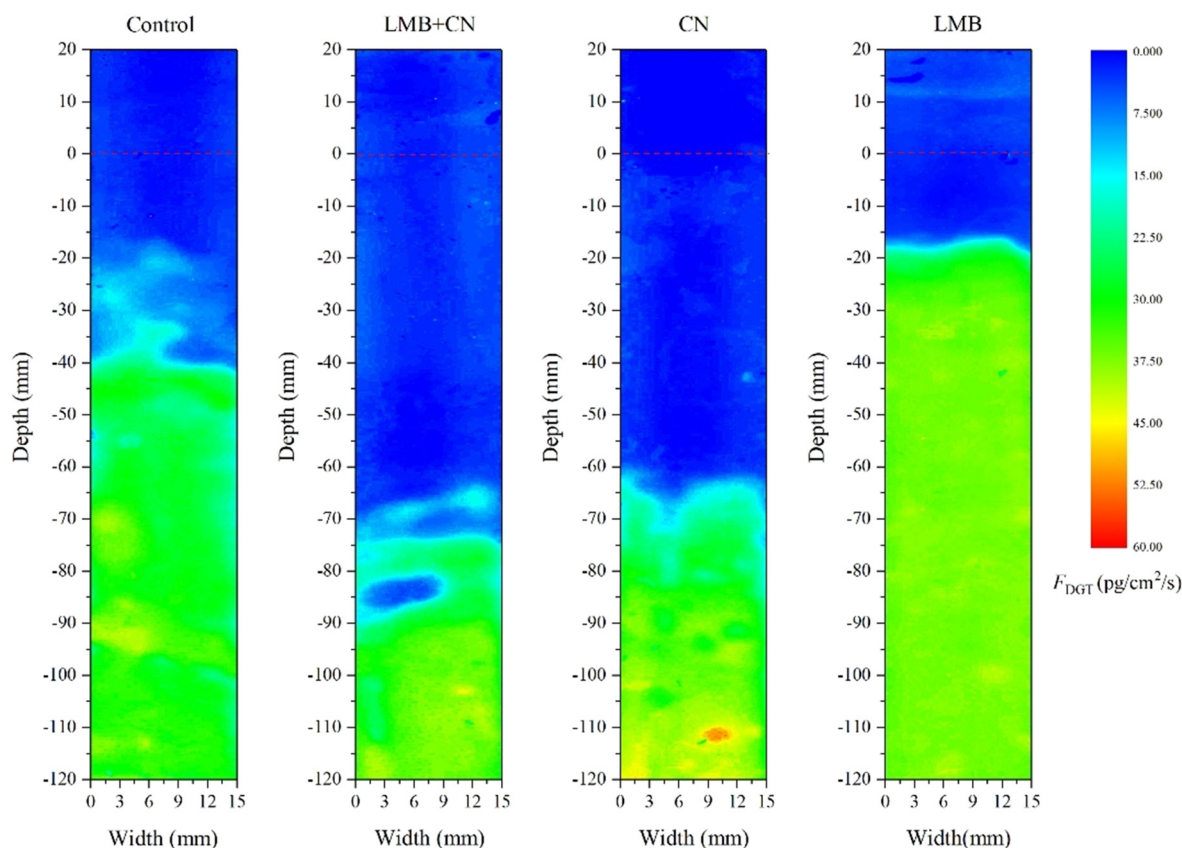**Fig. 9.** Changes in DGT-labile S(-II) in the sediment-water profiles after treatment for 68 days (the depth of 0 mm represents the sediment-water interface for CK and CN treatments and the capping layer-water interface for LMB and LMB + CN treatments, respectively).

and then increased from 14th to 68th days to reach 0.28 mg/L at the 68th day. At the deeper layers with depths of −10 mm, −20 mm, −30 mm and −40 mm, SRP decreased with time from 0.15 to 0.35 mg/L at the 68th day. These SRP values were lower than those of the control treatment. At the depth of −60 mm, SRP decreased with time from 2 to 62 h, and then increased from 62 h to 68th day. Its value was 2.20 mg/L, which was higher than that of the control treatment.

After the combined use of LMB and Ca(NO₃)₂ (LMB + CN treatment), the concentration of SRP was obviously lower than that of the control treatment at the depths from 0 to −50 mm during the whole incubation period. The concentrations of SRP were similar to those after LMB treatment at the SWI (0 mm depth), but the values were much lower in the deeper layer below the SWI. The concentration of SRP after LMB + CN treatment was similar to that after CN treatment. However, from the 336th hour (14th day), the values at the SWI (with mean value of 0.236 mg/L at the 14th day) were lower than those (with mean value of 0.514 mg/L at the 14th day) after CN treatment.

Fig. 11 compares the mean values of SRP concentration at the SWI from the four treatments. It can be seen that the SRP concentrations after CN and LMB + CN treatments were obviously lower than those of the control group and LMB treatment. Also, from the 336th hour (14th day), the SRP concentration of the LMB + CN treatment group was obviously lower than that of the CN treatment group.

After 68 days of treatment, the changes in DGT-labile P flux in the sediment are shown in Fig. 12A. By averaging the DGT-labile P flux levels, a one-dimensional image of the P flux was obtained, as shown in Fig. 12B. The flux of the CK treatment group increased with depth from 0 to −30 mm and was about 200 pg/cm²/s at the depth of −30 to −120 mm (Fig. 12). The DGT-labile P flux after LMB treatment was significantly lower than that after CK treatment at the depth of 20 to −20 mm; the average flux value of overlying water decreased from

32.31 pg/cm²/s to 16.06 pg/cm²/s while the average flux value at the depth of 0 to −20 mm in the sediment decreased from 54.09 pg/cm²/s to 14.44 pg/cm²/s (Table 1). The DGT-labile P flux for the CN treatment group was significantly lower than that for the CK treatment group at the depths of 0 to −75 mm and significantly higher than that for the CK treatment group in the overlying water and at the depths of −80 to −120 mm. The average value of DGT-labile P flux at the depth of 0 to −20 mm decreased to 34.40 pg/cm²/s; the average value at the depth of −20 to −80 mm decreased to 73.28 pg/cm²/s; the average value in the overlying water increased to 46.94 pg/cm²/s; and the average value at the depth of −80 to −120 mm increased to 389.2 pg/cm²/s. The average value of DGT-labile P flux after LMB + CN treatment decreased to 9.64, 11.26 and 65.06 pg/cm²/s in the overlying water, at the depths of 0 to −20 and −20 to −80 mm, respectively, which were lower than that after CN treatment.

3.7. Comparison of immobilization effects on sediment P

LMB treatment had a limited effect on mobile P in the sediment. The extent of action was mainly related to the additional dose of LMB and the amount of mobile P (Ding et al., 2018). Meis et al. (2013) found that the control of P released from sediments was achieved when the addition dose of LMB was 510 g/m². Lin et al. (2015) added 510 g/m² of LMB to the sediment and found that the amounts of loosely bound P and iron-bound P was reduced in the 20 mm surface mixed sediment (including the LMB layer) and about 50% of the mobile P was removed. When 260 g/m² of LMB was added, the removal proportion of mobile P in the 30 mm surface mixed sediment (including LMB layer) was only 14% (Lin et al., 2017). Wang et al. (2017) calculated the total amount of mobile P in the 40 mm surface sediment and added LMB at a dose of 200 LMB/P_mobile. It was found that the interstitial water SRP in 60 mm surface sediment was affected and mobile P in the 40 mm
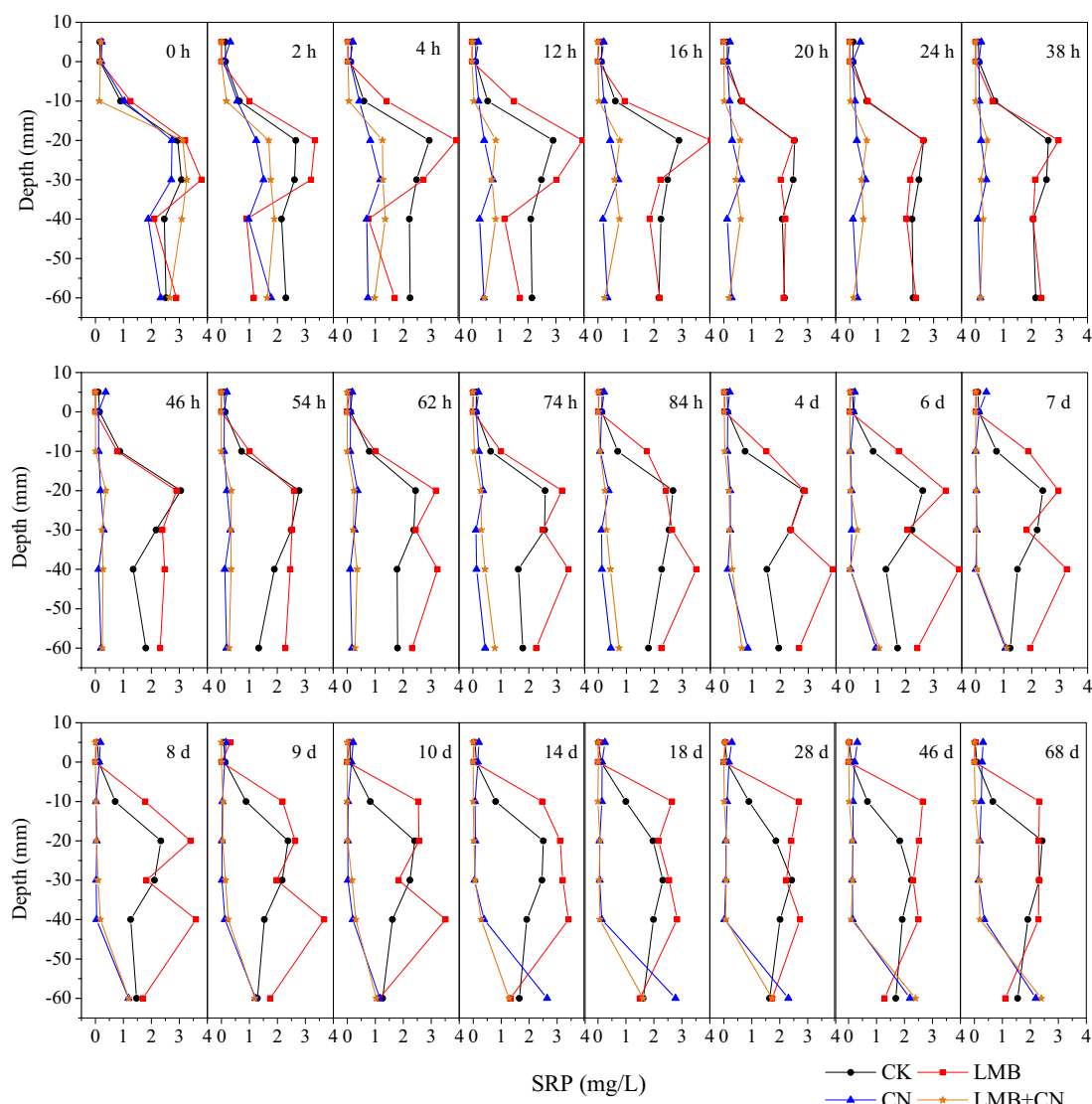
Fig. 10. Changes in concentrations of SRP in pore water with time in sediment-water profiles.
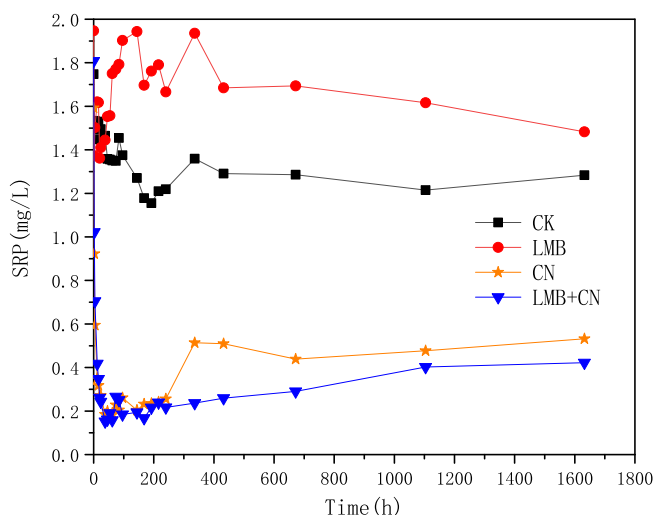

Fig. 11. Comparison of mean values of SRP concentration at the SWI from four treatments.

surface sediment was affected. In this study, the addition dose of LMB was about 120 LMB/P$_{mobile}$, and the pore water SRP was immobilized up to a depth of <10 mm. The effect on the DGT-labile P was limited to 20–30 mm (Fig. 12).

Compared to the overlying water addition method, the calcium nitrate sediment injection method can act on deep sediments more quickly. However, the injection process may disturb the sediment and cause desorption of solid-phase P and its release to the overlying water. In the present study, approximately 0.04 mg/L of DGT-labile P was released into the overlying water after the sediment was injected with a calcium nitrate dose of 45.3 g N/m^2. Lin et al. (2015) injected 61 g N/m^2 of calcium nitrate into the sediment and found that the concentrations of SRP and total P in the overlying water increased after 66 days. Lin et al. (2017) injected approximately 44 g N/m^2 calcium nitrate into the sediment and found that the SRP significantly increased on the 30th and 60th days. After the addition of calcium nitrate, many cracks appeared on the surface of the sediment and in the deep layer (Fig. 1). This may be because the addition of nitrate nitrogen promotes some reactions in the sediment and produces a large amount of gas (possibly nitrogen or nitrous oxide) to make the sediment loose. This may cause the release of endogenous P during the process of gas entering the overlying water (Lin et al., 2017).
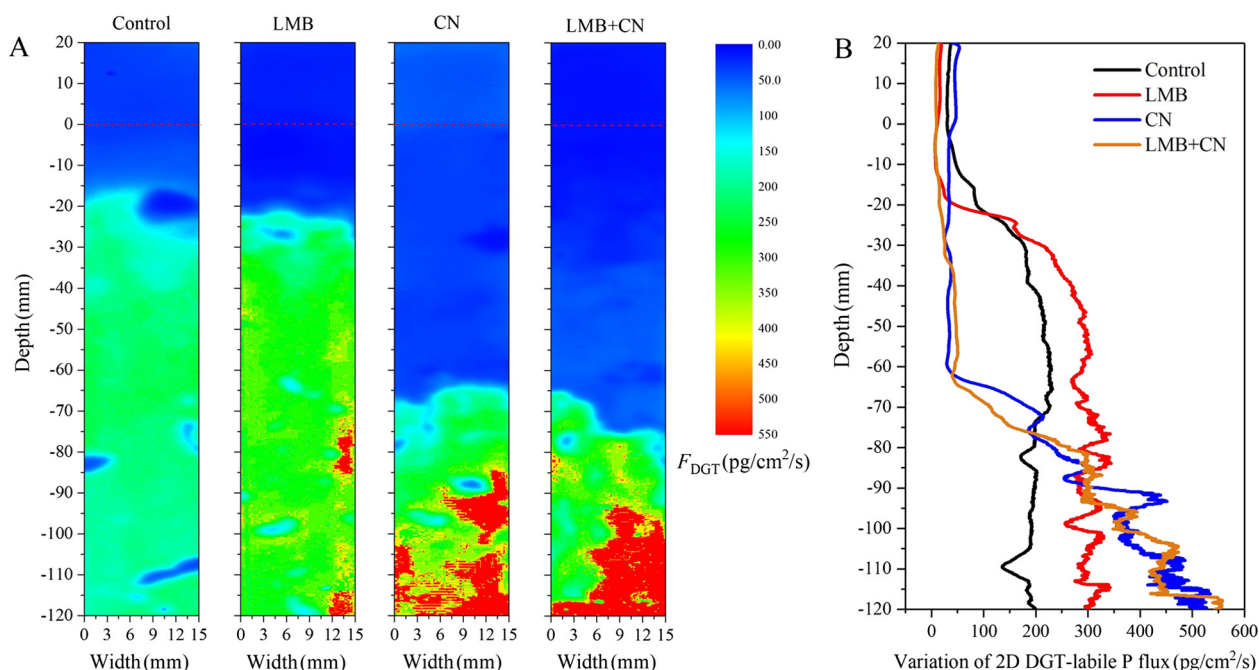
Fig. 12. Variation of 2D DGT-labile P flux (A) and horizontal average (B) in the sediment after treatment for 68 days.

The combined application of LMB and calcium nitrate can unite the advantages of the two agents to achieve better control of the SRP in overlying water and sediment P, thus suppressing the release of SRP from the sediment to the overlying water. The combined treatment affected the SRP in the 40 mm surface interstitial water and the DGT-labile P in the 60 mm sediment layers (Figs. 10, 12). This process can be simply described as: LMB acted as an adsorbent and barrier at the interface and converted the mobile P into a relatively stable form of P which is not easily disturbed by the environment; the calcium nitrate acted as a scavenging agent in the deep layer, and converted SRP in the pore water and the sediment existing in loosely bound state into a more stable iron-bound state, preventing the release of P from sediment.

After the combined application of LMB and calcium nitrate, SRP at the depth of −60 mm of sediment was first controlled. However, after a period of time, it rebounded and the concentration rose back to the level before treatment. This may be due to the strong desorption capacity of the sediment solid phase P. From the variation of dissolved nitrate nitrogen (Fig. 4), it was determined that the amount of NO_3^--N that can penetrate into the depth of −60 mm was the least and its consumption rate was the fastest, which returned to the pre-treatment level on the 8th day. When the nitrate nitrogen penetrating into the deep layer was completely consumed, desorption of solid phase P in the sediment played a leading role. Consequently, SRP in the pore water increased and the soluble Fe at the depth of −60 mm also increased (Figs. 7 and 10). Wang et al., (2016) found that when sufficient amount of nitrate was added, Eh value continued to rise. On the other hand, when the dose was insufficient, both pH and Eh rebounded. In this study, calcium

nitrate at a dose of 45.3 g N/m^2 was used to maintain the stability of P in the 40 mm surface sediment. Increasing or decreasing the dose may have effects on the range of action. Thus, in practice, the dose can be determined based on the nature of the sediment and the desired control effect.

4. Conclusions

The combined LMB + CN treatment significantly reduced the pH in the 20 mm surface sediment. The CN and LMB + CN treatments significantly increased Eh in the 30 mm surface sediment. All the LMB, CN, and LMB + CN treatments increased the ammonia nitrogen concentration in the pore water for a short time, but it eventually returned to the normal level relative to the control. The immobilization effect on sediment P extended to the upper 60 mm from the CN and the LMB + CN treatments, which were much thicker than 20 mm obtained by LMB treatment. Furthermore, LMB + CN treatment achieved the lowest concentration of SRP in the overlying water among the four treatments. Therefore, the proposed LMB + CN treatment is a better method for preventing the release of P from sediments by overcoming the drawbacks of the present methods.

Declaration of Competing Interest

The authors declare that they have no known competing financial interests or personal relationships that could have appeared to influence the work reported in this paper.

Table 1
Average DGT-labile P flux in the overlying water and different sediment layers.

Layer	DGT-labile P flux (pg/cm^2/s)			
	CK	LMB	CN	LMB + CN
20–0 mm	32.31	16.06	46.94	9.64
0 to −20 mm	54.09	14.44	34.40	11.26
−20 to −80 mm	196.6	260.4	73.28	65.06
−80 to −120 mm	184.5	301.8	389.2	386.7

References

Bostrom, B., Pettersson, K., 1982. Different patterns of phosphorus release from lake-sediments in laboratory experiments. Hydrobiologia 91-2 (1), 415–429.

Cao, T., Xie, P., Ni, L.Y., Wu, A.P., Zhang, M., Wu, S.K., Smolders, A.J.P., 2007. The role of NH$_4^+$ toxicity in the decline of the submersed macrophyte Vallisneria natans in lakes of the Yangtze River basin, China. Mar. Reshwater. Res. 58 (6), 581–587.

Copetti, D., Finsterle, K., Marziali, L., Stefani, F., Tartari, G., Douglas, G., Reitzel, K., Spears, B.M., Winfield, I.J., Crosa, G., D'Haese, P., Yasseri, S., Lurling, M., 2016. Eutrophication management in surface waters using lanthanum modified bentonite: a review. Water Res. 97, 162–174.

Cunningham, J.A., Rahme, H., Hopkins, G.D., Lebron, C., Reinhard, M., 2001. Enhanced in situ bioremediation of BTEX contaminated groundwater by combined injection of nitrate and sulfate. Environ. Sci. Technol. 35 (8), 1663–1670.

De Jonge, M., Teuchies, J., Meire, P., Blust, R., Bervoets, L., 2012. The impact of increased oxygen conditions on metal-contaminated sediments part II: effects on metal accumulation and toxicity in aquatic invertebrates. Water Res. 46 (10), 3387–3397.

De Lomas, J.G., Corzo, A., Gonzalez, J.M., Andrades, J.A., Iglesias, E., Montero, M.J., 2006. Nitrate promotes biological oxidation of sulfide in wastewaters: experiment at plant-scale. Biotechnol. Bioeng. 93 (4), 801–811.

Ding, S., Sun, Q., Xu, D., Jia, F., He, X., Zhang, C., 2012. High-resolution simultaneous measurements of dissolved reactive phosphorus and dissolved sulfide: the first observation of their simultaneous release in sediments. Environ. Sci. Technol. 46, 8297–8304.

Ding, S., Wang, Y., Xu, D., Zhu, C., Zhang, C., 2013. Gel-based coloration technique for the submillimeter-scale imaging of labile phosphorus in sediments and soils with diffusive gradients in thin films. Environ. Sci. Technol. 47, 7821–7829.

Ding, S., Sun, Q., Chen, X., Liu, Q., Wang, D., Lin, J., Zhang, C., Tsang, D.C.W., 2018. Synergistic adsorption of phosphorus by iron in lanthanum modified bentonite (Phoslock): new insight into sediment phosphorus immobilization. Water Res. 134, 32–43.

Dittrich, M., Gabriel, O., Rutzen, C., Koschel, R., 2011. Lake restoration by hypolimnetic Ca (OH)$_2$ treatment: impact on phosphorus sedimentation and release from sediment. Sci. Total Environ. 409 (8), 1504–1515.

Feibicke, M., 1997. Impact of nitrate addition on phosphorus availability in sediment and water column and on plankton biomass - experimental field study in the shallow brackish Schlei fjord (western Baltic, Germany). Water. Air. Soil. Poll. 99 (1–4), 445–456.

Foy, R.H., 1986. Suppression of phosphorus release from lake-sediments by the addition of nitrates. Water Res. 20 (11), 1345–1351.

Garcia-de-Lomas, J., Corzo, A., Portillo, M.C., Gonzalez, J.M., Andrades, J.A., Saiz-Jimenez, C., Garcia-Robledo, E., 2007. Nitrate stimulation of indigenous nitrate-reducing, sulfide-oxidising bacterial community in wastewater anaerobic biofilms. Water Res. 41 (14), 3121–3131.

Gołdyn, R., Podsiadłowski, S., Dondajewska, R., Kozak, A., 2014. The sustainable restoration of lakes-towards the challenges of the Water Framework Directive. Environ. Sci. Technol. 14 (1), 68–74.

Hansen, J., Reitzel, K., Jensen, H.S., Andersen, F.O., 2003. Effects of aluminum, iron, oxygen and nitrate additions on phosphorus release from the sediment of a Danish softwater lake. Hydrobiologia 492 (1–3), 139–149.

Hemond, H.F., Lin, K., 2010. Nitrate suppresses internal phosphorus loading in an eutrophic lake. Water Res. 44 (12), 3645–3650.

Hutchins, S.R., Miller, D.E., Thomas, A., 1998. Combined laboratory/field study on the use of nitrate for in situ bioremediation of a fuel-contaminated aquifer. Environ. Sci. Technol. 32 (12), 1832–1840.

Jiang, G.M., Sharma, K.R., Guisasola, A., Keller, J., Yuan, Z.G., 2009. Sulfur transformation in rising main sewers receiving nitrate dosage. Water Res. 43 (17), 4430–4440.

Kleeberg, A., Herzog, C., Hupfer, M., 2013. Redox sensitivity of iron in phosphorus binding does not impede lake restoration. Water Res. 47 (3), 1491–1502.

Kowalczewska-Madura, K., Dondajewska, R., Goldyn, R., Podsiadlowski, S., 2017. The influence of restoration measures on phosphorus internal loading from the sediments of a hypereutrophic lake. Environ. Sci. Pollut. R. 24 (16), 14417–14429.

Lang, P., Meis, S., Prochazkova, L., Carvaiho, L., Mackay, E.B., Woods, H.J., Pottie, J., Milne, I., Taylor, C., Maberly, S.C., Spears, B.M., 2016. Phytoplankton community responses in a shallow lake following lanthanum-bentonite application. Water Res. 97, 55–68.

Li, C., Ding, S., Yang, L., Wang, Y., Ren, M., Chen, M., Fan, X., Lichtfouse, E., 2019. Diffusive gradients in thin films: devices, materials and applications. Environ. Chem. Lett. 17, 801–831.

Lin, J., Qiu, P.H., Yan, X.J., Xiong, X., Jing, L.D., Wu, C.X., 2015. Effectiveness and mode of action of calcium nitrate and Phoslock® in phosphorus control in contaminated sediment, a microcosm study. Water. Air. Soil. Poll. 226 (10), 12.

Lin, J., Zhong, Y.F., Fan, H., Song, C.F., Yu, C., Gao, Y., Xiong, X., Wu, C.X., Liu, J.T., 2017. Chemical treatment of contaminated sediment for phosphorus control and subsequent effects on ammonia-oxidizing and ammonia-denitrifying microorganisms and on submersed macrophyte revegetation. Environ. Sci. Pollut. R. 24 (1), 1007–1018.

Liu, G.R., Ye, C.S., He, J.H., Qian, Q., Jiang, H., 2009. Lake sediment treatment with aluminum, iron, calcium and nitrate additives to reduce phosphorus release. J. Zhejiang. Univ-Sc. A 10 (9), 1367–1373.

Lu, R.K., 1999. Analytical Methods for Soil and Agricultural Chemistry. China Agricultural Science and Technology Press, Beijing.

Lurling, M., van Oosterhout, F., 2013. Case study on the efficacy of a lanthanum-enriched clay (Phoslock®) in controlling eutrophication in Lake Het Groene Eiland (The Netherlands). Hydrobiologia 710 (1), 253–263.

Lurling, M., Waajen, G., van Oosterhout, F., 2014. Humic substances interfere with phosphate removal by lanthanum modified clay in controlling eutrophication. Water Res. 54, 78–88.

Lurling, M., Mackay, E., Reitzel, K., Spears, B.M., 2016. Editorial - a critical perspective on geo-engineering for eutrophication management in lakes. Water Res. 97, 1–10.

Lurling, M., Waajen, G., Engels, B., van Oosterhout, F., 2017. Effects of dredging and lanthanum-modified clay on water quality variables in an enclosure study in a hyper-trophic pond. Water 9 (6), 24.

Meis, S., Spears, B.M., Maberly, S.C., Perkins, R.G., 2013. Assessing the mode of action of Phoslock® in the control of phosphorus release from the bed sediments in a shallow lake (Loch Flemington, UK). Water Res. 47 (13), 4460–4473.

Murphy, J., Riley, J.P., 1962. A modified single solution method for the determination of phosphate in natural waters. Anal. Chim. Acta 27, 31–36.

Na, Y.M., Park, S.S., 2004. Retardation of phosphate release from freshwater benthic sediments by application of ocher pellets with calcium nitrate. J. Environ. Sci. Heal. A. 39 (6), 1617–1629.

Nichols, D.S., Keeney, D.R., 1976. Nitrogen nutrition of myriophyllum-spicatum-uptake and translocation of N-15 by shoots and roots. Freshw. Biol. 6 (2), 145–154.

Rao, Q.Y., Deng, X.W., Su, H.J., Xia, W.L., Wu, Y., Zhang, X.L., Xie, P., 2018. Effects of high ammonium enrichment in water column on the clonal growth of submerged macrophyte Vallisneria natans. Environ. Sci. Pollut. R. 25 (32), 32735–32746.

Ripl, W., 1976. Biochemical oxidation of polluted lake sediment with nitrate: a new lake restoration method. Ambio 5, 132–135.

Rydin, E., Welch, E.B., 1999. Dosing alum to Wisconsin Lake sediments based on in vitro formation of aluminum bound phosphate. Lake. Reserv. Manage. 15 (4), 324–331.

Rydin, E., Kumblad, L., Wulff, F., Larsson, P., 2017. Remediation of a eutrophic bay in the Baltic Sea. Environ. Sci. Technol. 51 (8), 4559–4566.

Shao, M.F., Zhang, T., Fang, H.H.P., Li, X.D., 2011. The effect of nitrate concentration on sulfide-driven autotrophic denitrification in marine sediment. Chemosphere 83 (1), 1–6.

Spears, B.M., Mackay, E.B., Yasseri, S., Gunn, I.D.M., Waters, K.E., Andrews, C., Cole, S., De Ville, M., Kelly, A., Meis, S., Moore, A.L., Nurnberg, G.K., van Oosterhout, F., Pitt, J.A., Madgwick, G., Woods, H.J., Lurling, M., 2016. A meta-analysis of water quality and aquatic macrophyte responses in 18 lakes treated with lanthanum modified bentonite (Phoslock®). Water Res. 97, 111–121.

Tamura, H., Goto, K., Yotsuyanagi, T., Nagayama, M., 1974. Spectrophotometric determination of iron (II) with 1, 10-phenanthroline in the presence of large amounts of iron(III). Talanta 21, 314–318.

Tiren, T., Pettersson, K., 1985. The influence of nitrate on the phosphorus flux to and from oxygen depleted lake-sediments. Hydrobiologia 120 (3), 207–223.

Waajen, G., Pauwels, M., Lurling, M., 2017. Effects of combined flocculant - Lanthanum modified bentonite treatment on aquatic macroinvertebrate fauna. Water Res. 122, 183–193.

Wang, C.H., Jiang, H.L., 2016. Chemicals used for in situ immobilization to reduce the internal phosphorus loading from lake sediments for eutrophication control. Crit. Rev. Env. Sci. Tec. 46 (10), 947–997.

Wang, L.H., Li, J.G., Zhou, Q., Yang, G.M., Ding, X.L., Li, X.D., Cai, C.X., Zhang, Z., Wei, H.Y., Lu, T.H., Deng, X.W., Huang, X.H., 2014. Rare earth elements activate endocytosis in plant cells. P. Natl. Acad. Sci. USA. 111 (35), 12936–12941.

Wang, C.H., Jiang, H.L., Yuan, N.N., Pei, Y.S., Yan, Z.S., 2016. Tuning the adsorptive properties of drinking water treatment residue via oxygen-limited heat treatment for environmental recycle. Chem. Eng. J. 284, 571–581.

Wang, L., Long, X.X., Chong, Y.X., Yu, G.W., 2016. Potential risk assessment of heavy metals in sediments during the denitrification process enhanced by calcium nitrate addition: effect of AVS residual. Ecol. Eng. 87, 333–339.

Wang, Y., Ding, S.M., Wang, D., Sun, Q., Lin, J., Shi, L., Chen, M.S., Zhang, C.S., 2017. Static layer: a key to immobilization of phosphorus in sediments amended with lanthanum modified bentonite (Phoslock®). Chem. Eng. J. 325, 49–58.

Wang, C.H., Wu, Y., Wang, Y.Q., Bai, L.L., Jiang, H.L., Yu, J.H., 2018. Lanthanum-modified drinking water treatment residue for initial rapid and long-term equilibrium phosphorus immobilization to control eutrophication. Water Res. 137, 173–183.

Watsuntorn, W., Ruangchainikom, C., Rene, E.R., Lens, P.N.L., Chulalaksananukul, W., 2019. Comparison of sulphide and nitrate removal from synthetic wastewater by pure and mixed cultures of nitrate-reducing, sulphide-oxidizing bacteria. Bioresource Technol. 272, 40–47.

Xu, M.Y., Zhang, Q., Xia, C.Y., Zhong, Y.M., Sun, G.P., Guo, J., Yuan, T., Zhou, J.Z., He, Z.L., 2014. Elevated nitrate enriches microbial functional genes for potential bioremediation of complexly contaminated sediments. ISME 8 (9), 1932–1944.

Yamada, T.M., Sueitt, A.P.E., Beraldo, D.A.S., Botta, C.M.R., Fadini, P.S., Nascimento, M.R.L., Faria, B.M., Mozeto, A.A., 2012. Calcium nitrate addition to control the internal load of phosphorus from sediments of a tropical eutrophic reservoir: microcosm experiments. Water Res. 46 (19), 6463–6475.

Yan, L.L., Mu, X.Y., Han, B., Zhang, S.H., Qiu, C.H., Ohore, O.E., 2019. Ammonium loading disturbed the microbial food webs in biofilms attached to submersed macrophyte Vallisneria natans. Sci. Total Environ. 659, 691–698.

Yuan, G.X., Cao, T., Fu, H., Ni, L.Y., Zhang, X.L., Li, W., Song, X., Xie, P., Jeppesen, E., 2013. Linking carbon and nitrogen metabolism to depth distribution of submersed macrophytes using high ammonium dosing tests and a lake survey. Freshw. Biol. 58 (12), 2532–2540.

Zhang, M., Zhang, T., Shao, M.F., Fang, H.H.P., 2009. Autotrophic denitrification in nitrate-induced marine sediment remediation and Sulfurimonas denitrificans-like bacteria. Chemosphere 76 (5), 677–682.

Zhang, X.T., Sun, F.L., He, J.J., Xu, H.B., Cui, F.Y., Wang, W., 2017. Robust phosphate capture over inorganic adsorbents derived from lanthanum metal organic frameworks. Chem. Eng. J. 326, 1086–1094.

Zhuang, K., Shi, D.L., Hu, Z.B., Xu, F.L., Chen, Y.H., Shen, Z.G., 2019. Subcellular accumulation and source of O$_2$ and H$_2$O$_2$ in submerged plant Hydrilla verticillata (L.f.) Royle under NH4+-N stress condition. Aquat. Toxicol. 207, 1–12.